Atmospheric rivers' direction over land matters for characterising its impact in New Zealand

Jingxiang Shu[1]*, Asaad Y. Shamseldin[1], Evan Weller[2]

[1]Department of Civil and Environmental Engineering, The University of Auckland, Private Bag 92019, Auckland Mail Centre, Auckland 1142, New Zealand.

[2] School of Environment, The University of Auckland, Private Bag 92019, Auckland Mail Centre, Auckland 1142, New Zealand.

Corresponding author: Jingxiang Shu (jshu987@aucklanduni.ac.nz)

Key Points:

- ARs direction and orography determine the favourable locations of heavy rainfall in New Zealand

- Most heavy rainfall produced by weak and short ARs are easterly directed over eastern regions

- AR direction may consider developing a more applicable AR-impact ranking scale for eastern regions in New Zealand

Abstract

Atmospheric Rivers (ARs) are filamentary channels of strong poleward water vapour transport in the midlatitudes. Recent studies have demonstrated the significant role of ARs in New Zealand's water resources and extreme precipitation events. Motivated by a recently proposed AR-impact ranking scale in the USA to enhance the communication between scientific communities and water sectors, here the characteristics of AR events with peak daily rainfall greater than 100 mm over 5 divided sectors are further investigated, and the AR-impact ranking scale is evaluated for the applicability for such events in New Zealand. Previous studies have found that the windward side along coastlines favours locally high rainfall. As such, we show that the strength and duration of those AR events also vary with event direction, and NW-AR events are normally stronger and longer than those of other directions throughout the country. However, over the eastern areas, most of those events are easterly directed and produce anomalously high rainfall, despite being ranked as "Weak AR" events based on the current AR-impact ranking scale. It is found that easterly directed ARs originating from the west make landfall along the eastern coastline from the ocean (i.e., from the east) or simply the onshore flow. Therefore, our results suggest that localised ranking scale or considering more parameters, such as AR overland direction, might help improve the AR-impact ranking scale applicability over eastern regions in New Zealand.

1 Introduction

New Zealand is a long and narrow country surrounded by ocean spanning from 34°S to 47°S in the midlatitudes. Mountain ranges in the country trend southwest-northeast peaking at 3764 m. Main precipitation-generating weather

1

systems are cyclones in the Tasman Sea and tropical cyclones from the north passing or near northern regions of the country, and fronts and depressions within the band of westerlies to the south of the country (Salinger, 1980). In combination with orographic uplift, there are 4 main rainfall mechanisms common throughout the country: uplift within cold fronts and cyclones embedded in the westerlies; enhanced rainfall on the windward side of mountain ranges due to orographic uplift; convective rainfall due to summer heating in eastern regions; subtropical frontal systems from the north (Tait & Fitzharris, 1998). Overall, anomalously high precipitation tends to distribute along the windward side of most coastal areas than the leeward side due to the orographic uplift on the windward side along most coastlines (Salinger, 1980).

Atmospheric rivers (ARs) are long and narrow channels of enhanced poleward water vapour transport in the midlatitudes (Newell et al., 1992; Newell & Zhu, 1994; Ralph et al., 2004, 2005, 2018; Zhu & Newell, 1994, 1998). Their presence is often tied with frontal systems (Liu et al., 2021; Ralph et al., 2004, 2005; Zhu & Newell, 1998) and cyclones (Cordeira et al., 2013; Guo et al., 2020; Ralph et al., 2004, 2005; Sodemann & Stohl, 2013; Zhang et al., 2019; Zhou & Kim, 2019; Zhu & Newell, 1994). The AR-related hazards and benefits in New Zealand have been recently investigated (Kingston et al., 2016, 2021; Porhemmat et al., 2020; Prince et al., 2021; Reid et al., 2021; Shu, Shamseldin, & Weller, 2021). Generally, ARs are a significant contributor to water resources and responsible for many extreme precipitation events on the western side of mountain ranges throughout the country because the orographic uplifting effect and ARs commonly make landfall from a northwest direction (Porhemmat et al., 2020; Prince et al., 2021; Shu, Shamseldin, & Weller, 2021). Additionally, a framework using AR's duration and the peak magnitude of AR events to characterise AR's strength and impact (Ralph et al., 2019) was evaluated recently in New Zealand (Prince et al., 2021).

However, the authors noted that in some cases, AR events with a short duration (<24 hours) or weak magnitude (<250 kg m^{-1} s^{-1}) also lead to heavy rainfall events (Prince et al., 2021). It is also noteworthy that ARs can approach the east coast from a northeast or southeast direction in some cases (Prince et al., 2021; Shu, Shamseldin, & Weller, 2021). As noted in Reid et al. (2021), at least 80% of the top historical rainfall events showing the association with AR events for some rain sites located on the eastern side of mountain ranges, despite the percentage of AR-induced extreme rainfall events being relatively low in such areas (Shu, Shamseldin, & Weller, 2021). Considering the diverse topography (Figure 2) and the windward side of mountain ranges being favourable for anomalously high precipitation in New Zealand (Salinger, 1980), the impact of AR-induced precipitation is very likely to be related to an AR's over-land direction instead of only the AR intensity and duration. For regions with diverse topography and varied catchment orientations in other countries, previous studies have found that the direction of landfalling ARs plays a significant role in modulating the distribution of extreme precipitation events (Hecht & Cordeira, 2017; Hughes et al., 2014; Neiman et al., 2013) and flood occurrence in different catchments

(Griffith et al., 2020), for instance, ARs with similar strength but different directions can cause floods in different catchments over western Washington (Neiman et al., 2011).

As such, the purpose of this paper is to examine the role of AR over-land directions in determining the heavy rainfall event distribution and the AR's impact in terms of the associated disasters over New Zealand, and further to evaluate the applicability of the AR-impact ranking scale in the country on the aspect of the AR-event direction overland. This concept is motivated by the idea of using the AR-impact ranking scale developed by Ralph et al. (2019) to enhance the communication between scientific communities and the broader audience (water managers, the public, policymakers, media.) in terms of AR-related benefits and hazards. Given the complex topography and the 4 main rainfall mechanisms in New Zealand, we hypothesise that including AR over-land directions might help develop a more applicable AR-impact ranking scale.

This is the first study to evaluate the strength and duration of AR activities that produce extreme rainfall and the applicability of the AR-impact ranking scale concerning AR over-land directions in New Zealand, and it is organised as follows. Section 2 describes the collected data, AR detection algorithm, AR-impact ranking scale, AR-rain identification method, and divided sectors in terms of "AR impact" and orography, according to (Shu, Shamseldin, Weller, et al., 2021). Section 3 presents results regarding the characteristics of landfalling ARs that lead to heavy rainfall in different landfall directions in the divided sectors. Section 4 evaluates the applicability of the AR-impact raking scale and presents several case studies to demonstrate a need to develop a regional localised ranking scale or more parameters considered to improve the applicability of the AR-impact ranking scale in New Zealand. Finally, Section 5 provides a summary and conclusions.

2 Data and Methods

2.1 Data

AR detection is based on the Eulerian framework (Blamey et al., 2018; Lavers et al., 2012; Nayak & Villarini, 2017) using the integrated water vapour transport (IVT) calculated by:

$$\text{IVT} = \sqrt{\left(\frac{1}{g}\int_{1000\text{hPa}}^{300\text{hPa}}\text{qu dp}\right)^2 + \left(\frac{1}{g}\int_{1000\text{hPa}}^{300\text{hPa}}\text{qv dp}\right)^2}, (1)$$

where g is the gravitational acceleration (9.81 m s^{-2}), q is specific humidity (kg kg^{-1}), u and v are zonal and meridional wind vectors (m s^{-1}), respectively, and dp is the pressure difference between two adjacent atmospheric pressure levels (hPa). 6-hourly specific humidity and wind vectors through 20 vertical pressure levels (1000hPa-300hPa) were retrieved from the Medium-Range Weather Forecasts (ECMWF), a most recent high-resolution atmospheric reanalysis dataset, namely ERA5 (Hersbach et al., 2020) from 1950 to 2021 with a 0.25° spatial resolution over the 0-70°S and 100°E-120°W domain. Station-based daily rain-

fall amounts were obtained from New Zealand's national climate database web system managed by the National Institute of Water and Atmospheric Research (NIWA), and 644 rain sites with at least 30 years of complete daily records from 1950-2021 were obtained.
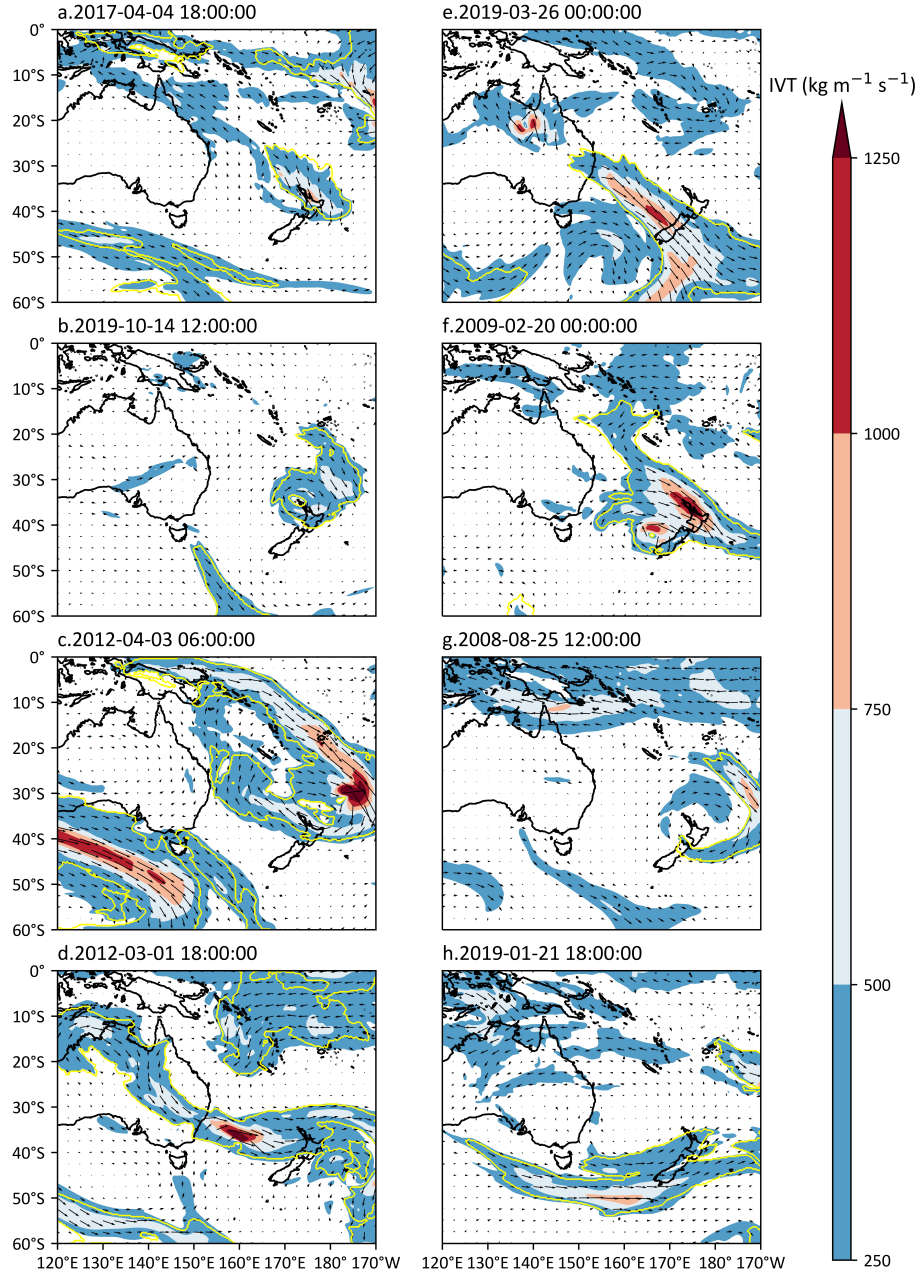
Figure 1. Key examples of ARs with different landfall directions. Over North Island: (a) NW-AR events, (b) NE-AR events, (c) SE-AR events, (d) SW-AR events. Over South Island: (e) NW-AR events, (f) NE-AR events throughout the eastern regions, (g) SE-AR events, (h) SW-AR events. The yellow lines indicate AR boundaries, and time is in UTC.

2.2 AR detection

This study employed a widely-used AR detection algorithm developed by Guan and Waliser (2015), which includes a set of conditions on the grided IVT to identify AR objects every time step. The AR object is the instantaneous area (a collection of grid cells) that meets the defined AR detection conditions. The detection conditions include varied monthly thresholding of grided IVT magnitude, the AR object poleward direction check, IVT direction coherence within the AR object, and the AR-object geometry. Detailed AR detection procedures and conditions are provided in Guan and Waliser (2015). This algorithm was only the one that has been validated from the dropsonde observations for the AR intensity and geometry and has been widely used as a benchmark in different regions for regional-specific AR detection algorithm development (Gershunov et al., 2017; Pan & Lu, 2019; Reid et al., 2020). Archived landfalling AR dates from this algorithm shows over 90% agreement with other regional-specific AR detection techniques (Gorodetskaya et al., 2014; Guan et al., 2018; Lavers et al., 2012; Neiman et al., 2008; Ralph et al., 2019; Shields et al., 2018). Figure 1 shows 8 landfalling ARs approaching the country with different landfall directions.

2.3 AR-impact ranking scale

An AR-impact ranking scale was initially developed by Ralph et al. (2019) to categorise AR's strength and impact by the AR-event peak IVT magnitude and duration over the location of interest. Briefly, the IVT and duration intervals for categorising an AR event rank is 250 kg m^{-1} s^{-1} and 24 hours, respectively. A detailed description of the ranking scale is in Ralph et al. (2019). It should be noted that the AR-impact ranking scale used in this study is slightly different (Table 1) since the AR detection algorithm by Guan and Waliser (2015) enables ARs with IVT less than 250 kg m^{-1} s^{-1}. In this study, AR events with a peak IVT magnitude less than 250 kg m^{-1} s^{-1} were ranked as "Weak AR" events.

Table 1. AR-impact ranking scale used in this study for New Zealand landfalling AR events, modified from Ralph et al. (2019)

AR-event peak IVT (kg m^{-1} s^{-1})	Duration of AR event (hours)		
	24	>24-48	>48
250	Weak AR	Weak AR	Weak AR
>250-500	Weak AR	Cat1 AR	Cat2 AR
>500-750	Cat1 AR	Cat2 AR	Cat3 AR

5

AR-event peak IVT (kg m^{-1} s^{-1})	Duration of AR event (hours)		
>750-1000	Cat2 AR	Cat3 AR	Cat4 AR
>1000-1250	Cat3 AR	Cat4 AR	Cat5 AR
>1250	Cat4 AR	Cat5 AR	Cat5 AR

2.4 AR-induced rainfall events

We modified the method used to identify AR-induced rainfall events in Shu, Shamseldin, & Weller (2021). Based on the geographical coordinate of the 4 grid points enclosing a rain gauge, the date and time that all 4 points simultaneously detected AR activities were referred to an AR event at that date and time for that rain gauge. The start and end date and time of each AR event were then obtained, and duration was computed accordingly. The areal mean IVT and mean direction at 4 points of each time step(s) of each AR event were computed, and the peak areal mean IVT and mean direction over all time step(s) within the AR-event duration were further computed. Moreover, the peak daily rainfall amounts and the standardised index of each AR event were obtained, and the index was calculated as:

Standardised index $= \frac{x - \overline{x}}{S}$, (2)

where x is the AR-event peak daily rain amount, $\overline{x}$ is the mean daily rainfall through the entire dataset (>0 mm), S is the standard deviation of daily rain. Following the work done by Shu, Shamseldin, & Weller (2021) and Shu, Shamseldin, Weller, et al. (2021), areas that experience higher AR's contribution to annual rainfall tend to see a higher proportion of top 10% heavy rainfall events linked with ARs. To further evaluate the applicability of the AR-impact ranking scale in New Zealand, the country was divided into 5 sectors considering the "AR impact" and orographic control on precipitation (Figure 2). To evaluate the applicability of the AR-impact ranking scale on extreme rainfall events, we only consider events with peak rainfall >100 mm linked with AR events. Additionally, all AR events with peak rainfall over 100 mm are over 18 hours.
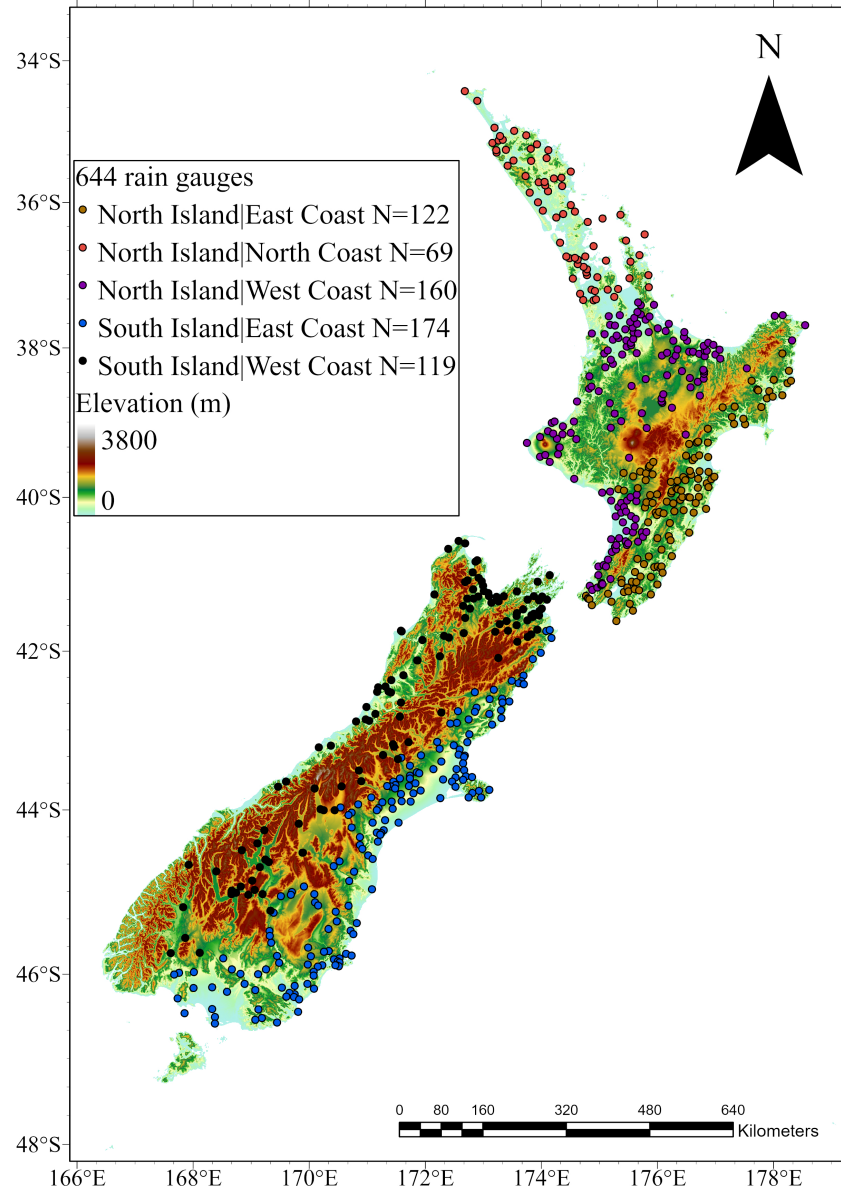
Figure 2. The spatial distribution of the 5 regional sectors and 644 rain sites used in the study.

3 Anomalously high rainfall in relation to AR landfall direction

Figure 3 shows the percentage of AR events with peak rainfall over 100 mm in terms of AR event mean direction, and Table 2 illustrates the sample size of AR events for each direction over the rain site. High rainfall events are

dominated by easterly directed ARs, with 49.3% of NE direction and 32.2% of SE direction for the East Coast of North Island, while the West Coast of North Island sees more high rainfall events related to westerly directed ARs (73.4% of NW direction). In North Island, the weather system on North Coast is more likely to be governed by westerlies and subtropical cyclones (Salinger, 1980). Hence, this group sees 41.3% of NW- and 57.2% of NE- AR events causing high rainfall. Likewise, it is more likely to see high rainfall events related to NW-AR events for the West Coast, while the East Coast sees a higher probability of easterly AR events leading to high rainfall (21.6% of NE-AR events and 33% of SE-AR events). In some cases, NW-ARs can pass mountain ranges from the West Coast, causing high rainfall in the East Coast (40.2% of NW-AR events).

Table 2. AR events lead to peak daily rain over 100 mm count

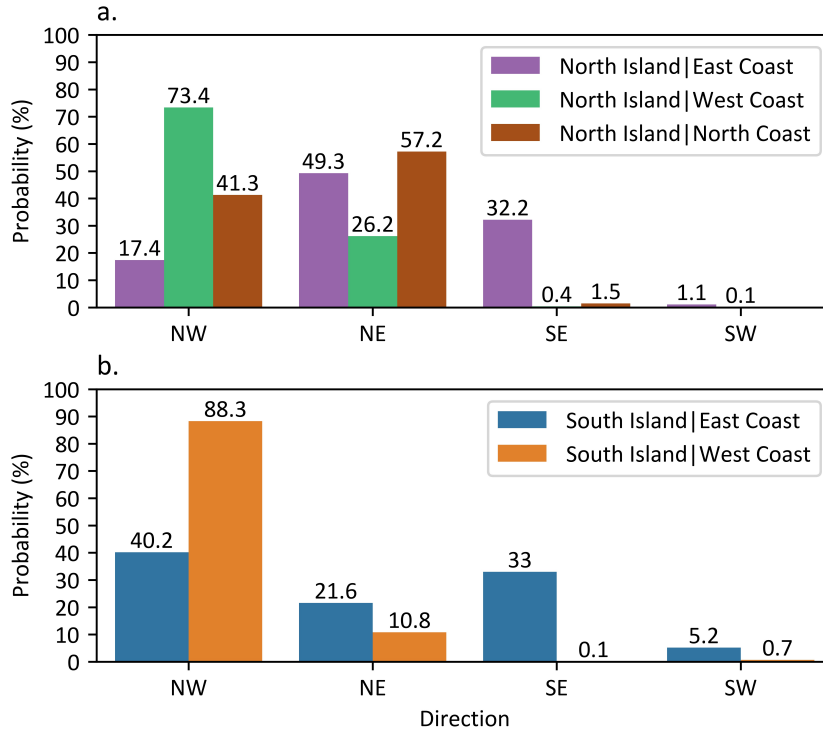|	NW	NE	SE	SW	Total
North Island East Coast	47	133	87	3	270
North Island West Coast	813	290	4	1	1108
North Island North Coast	166	230	6	0	402
South Island East Coast	39	21	32	5	97
South Island West Coast	2086	256	3	17	2362

Figure 3. Probability of AR-induced heavy rainfall events with peak daily rain over 100 mm on 4 directions in each regional sector for the (a) North Island and (b) South Island.

Figure 4 shows the peak IVT magnitude, duration, peak rainfall and standardised rainfall index during each detected AR event. As expected, ARs that lead to high rainfall events are generally stronger with longer duration in the NW direction than other directions over the entire country as westerlies largely dominate the weather year-round. Daily rainfall over 100 mm is less common for the East Coast of both Islands and North Coast of North Island (Table 2), and the median of the standardised rainfall index is relatively higher than that of the West Coast regardless of the AR event direction. However, it is noteworthy that NE-AR and SE-AR events for the East Coast can cause heavy rainfall with larger anomalies than the West Coast, despite being weaker and shorter than NW-AR events.
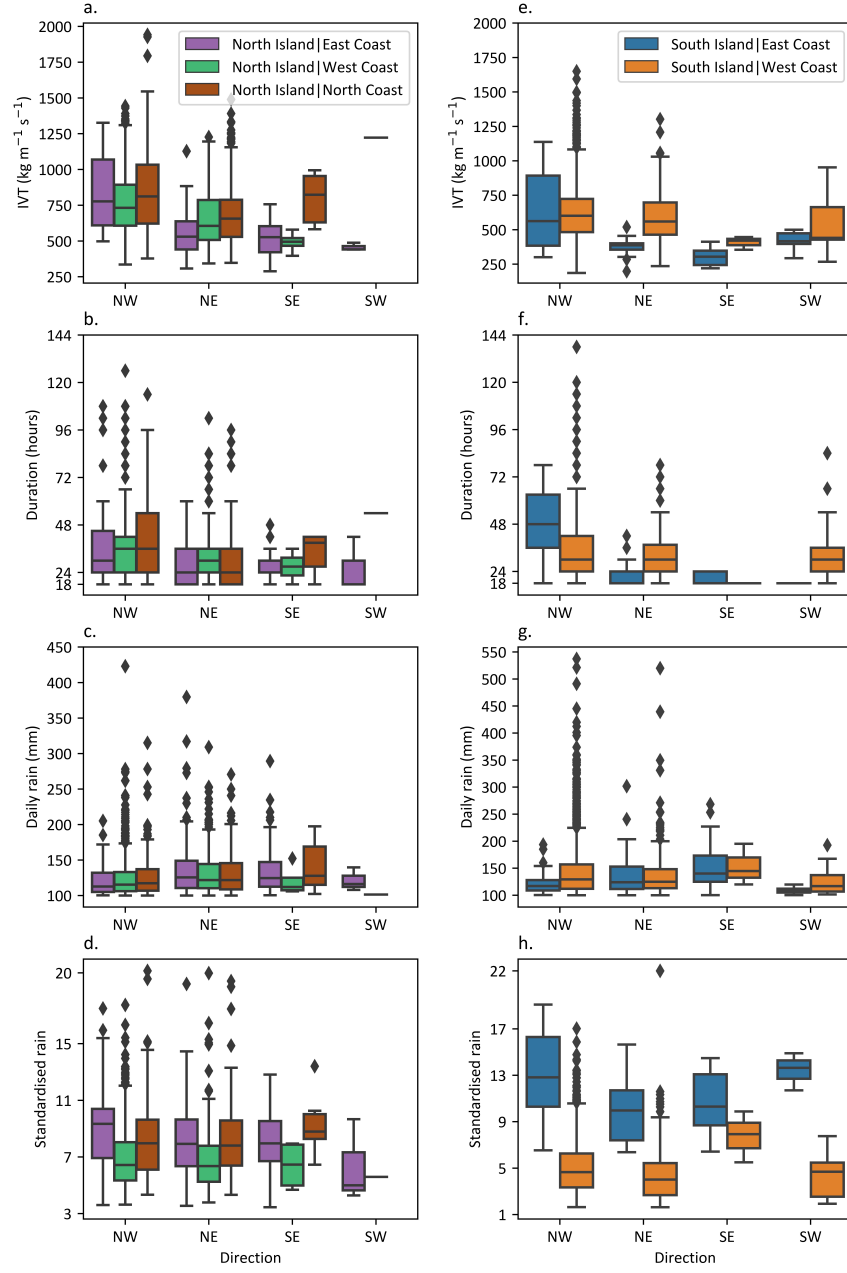
Figure 4. Characteristics of AR events with peak daily rain over 100 mm and standardised peak daily rain on 4 directions in each regional sector. AR events over North Island: (a) Peak IVT magnitude, (b) Duration, (c) Peak daily rain, (d) Standardised peak daily rain. (e) – (h) Same as (a) – (d) but for South Island.

4 AR-impact ranking scale assessment

We further calculated the probability of ARs on each category in each direction for ARs events with peak rainfall over 100 mm. Interestingly, most ARs that lead to anomalously high rainfall are ranked as "Weak ARs" on the NE direction for the East Coast of North Island and the NE and SE directions for the East Coast of South Island (Figure 5). Table 3 shows three AR events that produced anomalously high rainfall but were categorised as "Weak AR" events over the East Coast areas, and one event with "Cat3" and "Cat4" AR events over the West Coast and North Coast of North Island but "Weak AR" events for the East Coast of South Island. Figures S1-S3 illustrate these 3 events.
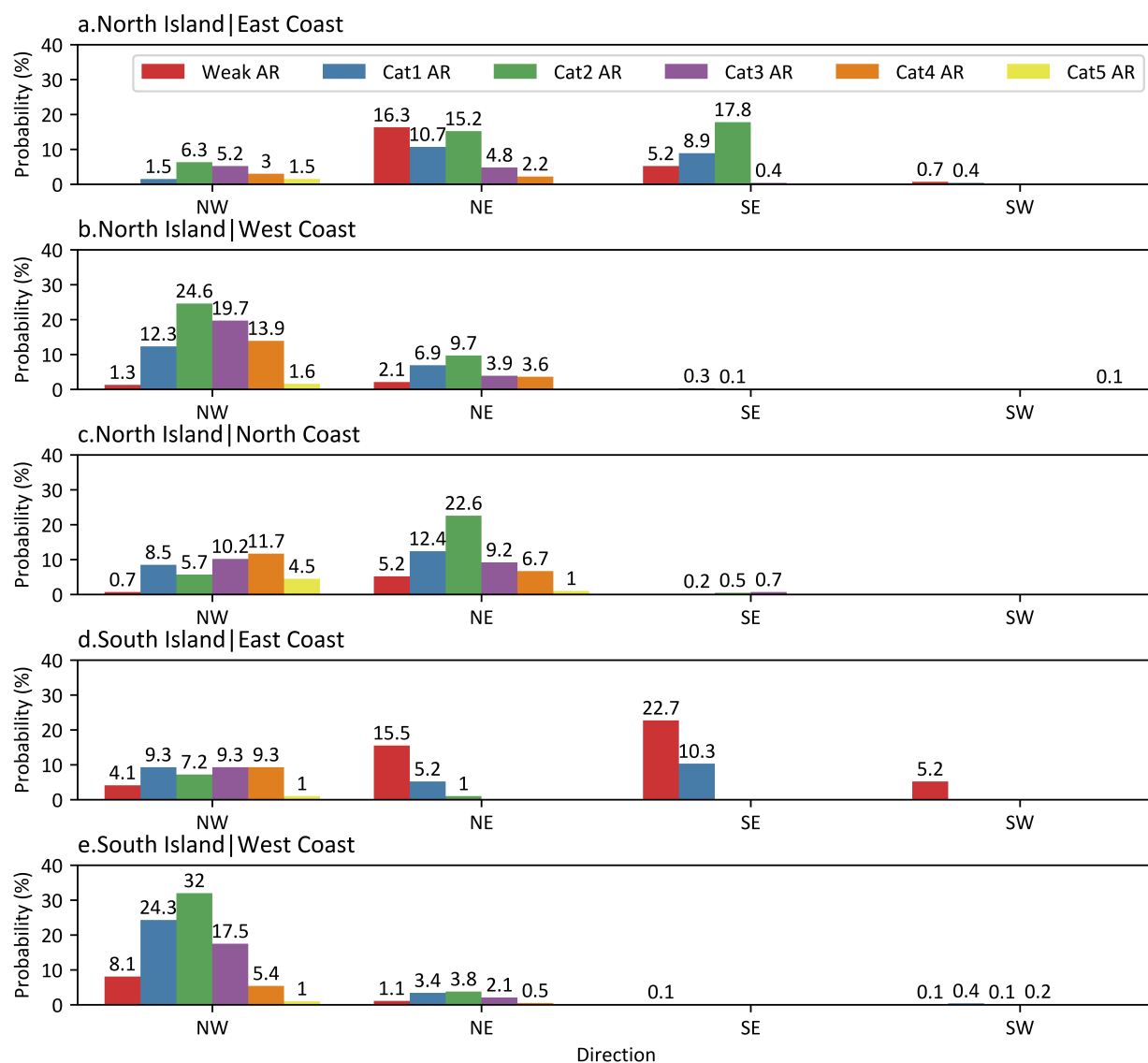
Figure 5. Probability of categorised AR events with peak daily rain over 100 mm on 4 directions for 5 regional sectors.

Several regions in North Island were affected by severe storms and strong winds from 15 to 16 October 2019, although weak AR events were detected (Figure S1). On 15 October 2019, the northern and western North Island were affected, several schools and State Highway 25 were closed due to flooded roads in the Coromandel region and power was off at more than 100 homes due to wind gusts in Auckland city and Tauranga region (NZ Herald, 2019). Later on 16 October, anomalously high rainfall was concentrated on the east of the North Island

(Table 3), with flooding in the Hawkes Bay region (Deguara & Forrester, 2019). From 19 to 21 February 2009, the entire country experienced heavy rainfall, high winds, floods, and one woman died in a car accident due to heavy rainfall (NIWA, 2009). North Island and South Island experienced AR events in a different category (Figure S2 and Table 3). However, clearly "Weak AR" events in the East Coast of South Island caused rainfall with high anomaly greater than that by "Cat3" or "Cat4" AR events in the West Coast of North Island (Table 3). Furthermore, the East Coast of North Island experienced "Weak AR" events from 24 to 27 August 2008 (Figure S3 and Table 3), heavy rainfall caused landslides and flooding around northern Canterbury and Marlborough region, and flood damage was expected to cost over $7 million New Zealand dollars in total for the 2 regions (NIWA, 2008).

Table 3. AR events ranked as "Weak AR" events but led to anomalously high rainfall in eastern regions

Rain site(s) sector	Start date (New Zealand Daylight Time)	Mean direction	AR event category	Peak rainfall (mm)	Standardised rainfall	No of rain sites
North Island East Coast	October 2019	NE	weak	-133	-7	
South Island East Coast	February 2009	NE	weak	-123.5	-12.1	
North Island North Coast 1 North Island West Coast	February 2009	NW	Cat4 1 Cat3	-103	-5.2	
South Island East Coast	August 2008	SE	weak	-286.4	-13.9	

5 Conclusions

This study evaluates the applicability of the AR-impact ranking scale in New Zealand developed by Ralph et al. (2019). Characteristics of AR events that lead to heavy rainfall events were investigated. Note that in this study, we only consider AR events with a peak rainfall over 100 mm. Overall, landfalling ARs were detected based on the widely used AR detection algorithm by Guan and Waliser (2015) and the method used in Shu, Shamseldin, & Weller (2021) to identify AR-event rainfall was modified to obtain characteristics of AR events among 644 rain gauges, including duration, peak IVT magnitude, mean direction, category, peak daily rain and its standardised index of each AR event among rain gauges. Following Shu, Shamseldin, Weller, et al. (2021), the country was divided into 5 regional sectors in terms of "AR impact" and orographic control on local weather: the East Coast and the West Coast of both islands, as well as the North Coast of North Island. With this regard, the AR-induced heavy rainfall pattern in relation to the AR-event mean direction and the performance of the AR-impact ranking scale were investigated.

AR's direction, combined with mountain ranges' orientation, is presumed to play a prominent role in determining the spatial distribution of anomalously high rainfall events over New Zealand. In this regard, we found that most AR-induced heavy rainfall events are likely to associate with the westerlies, namely NW ARs over the West Coast of the country (Table 2), while the North Coast and East Coast areas are more likely to see easterly ARs bring heavy rainfall as these ARs are associated with cyclones embedded in westerlies and tropical cyclones (Figures 1b-c and f-g, S1-S3). We further investigated the characteristics of AR events that generate heavy rainfall over 5 regional sectors. Interestingly, particularly for the East Coast areas over the country, most AR-induced heavy rainfall events are easterly directed, although they are of relatively low IVT magnitude and short duration when compared to NW AR events, and most of them are ranked as "Weak AR" events.

The major precipitation-generating weather systems are the westerlies and cyclones over the Tasman Sea and/or the tropical region due to the geographical location of New Zealand (Salinger, 1980; Tait & Fitzharris, 1998). Compared to USA's landmass, New Zealand is a long and narrow country surrounded by ocean, enabling ARs to approach the east coastline either by inland penetration from northwest or easterly directed ARs but originating from the northwest (Figures 1 and S1-S3). Presumably, the AR-impact ranking scale performs well for the country's West Coast because it is on the windward side as NW-AR events are generally stronger and longer (Figures 4-5). However, the East Coast can also experience extreme rainfall events as it becomes the windward side when easterly ARs make landfall, even though those ARs are generally weaker and shorter than NW-AR events. With this regard, the orographic lifting effect can enhance the AR-induced precipitation on either the western or eastern mountain ranges, depending on the AR's over-land direction. Therefore, a localised AR-impact raking scale or a ranking scale considering the direction might be more applicable for the eastern regions over the country. We will study this in more detail in the future.

Additionally, a further investigation of AR sources and the association between ARs and dynamical weather processes, such as cyclones, might be useful for a more applicable AR-impact ranking scale employed in the country. In some cases, ARs appear to be rotated and strongly associated with cyclones (Figures 1 and S1-S3). Future studies could focus on more characteristics of landfalling ARs and weather dynamics related to them over the eastern coast to improve the applicability of the AR-impact ranking scale in the country.

Data Availability Statement

Data used in this study were obtained freely online (registration required):

ERA5 hourly data on pressure levels from 1950 to 1978 (preliminary version): https://cds.climate.copernicus.eu/cdsapp#!/dataset/reanalysis-era5-pressure-levels-preliminary-back-extension?tab=overview

ERA5 hourly data on pressure levels from 1979 to present:

https://cds.climate.copernicus.eu/cdsapp#!/dataset/reanalysis-era5-pressure-levels?tab=overview

Daily rainfall: https://cliflo.niwa.co.nz/pls/niwp/wgenf.genform1

References

Blamey, R. C., Ramos, A. M., Trigo, R. M., Tomé, R. & Reason, C. J. C. (2018). The Influence of Atmospheric Rivers over the South Atlantic on Winter Rainfall in South Africa. *Journal of Hydrometeorology*, *19*(1), 127–142. https://doi.org/10.1175/JHM-D-17-0111.1Cordeira, J. M., Ralph, F. M. & Moore, B. J. (2013). The Development and Evolution of Two Atmospheric Rivers in Proximity to Western North Pacific Tropical Cyclones in October 2010. *Monthly Weather Review*, *141*(12), 4234–4255. https://doi.org/10.1175/MWR-D-13-00019.1Deguara, B. & Forrester, G. (2019). *Flood damage, sodden backyards and playgrounds: More heavy rain to batter North Island.* https://www.stuff.co.nz/national/116611486/heavy-rain-batters-north-island-again-temperatures-drop-in-the-southGershunov, A., Shulgina, T., Ralph, F. M., Lavers, D. A. & Rutz, J. J. (2017). Assessing the climate-scale variability of atmospheric rivers affecting western North America. *Geophysical Research Letters*, *44*(15), 7900–7908. https://doi.org/10.1002/2017GL074175Gorodetskaya,

I. V., Tsukernik, M., Claes, K., Ralph, M. F., Neff, W. D. & Van Lipzig, N. P. M. (2014). The role of atmospheric rivers in anomalous snow accumulation in East Antarctica. *Geophysical Research Letters*, *41*(17), 6199–6206. https://doi.org/10.1002/2014GL060881Griffith, H. V., Wade, A. J., Lavers, D. A. & Watts, G. (2020). Atmospheric river orientation determines flood occurrence. *Hydrological Processes*, *34*(23), 4547–4555. https://doi.org/10.1002/hyp.13905Guan, B. & Waliser, D. E. (2015). Detection of atmospheric rivers: Evaluation and application of an algorithm for global studies. *Journal of Geophysical Research: Atmospheres*, *120*(24), 12514–12535. https://doi.org/10.1002/2015JD024257Guan, B., Waliser, D. E. & Martin Ralph, F. (2018). An intercomparison between reanalysis and dropsonde observations of the total water vapor transport in individual atmospheric rivers. *Journal of Hydrometeorology*, *19*(2), 321–337. https://doi.org/10.1175/JHM-D-17-0114.1Guo, Y., Shinoda, T., Guan, B., Waliser, D. E. & Chang, E. K. M. (2020). Statistical relationship between atmospheric rivers and extratropical cyclones and anticyclones. *Journal of Climate*, *33*(18), 7817–7834. https://doi.org/10.1175/JCLI-D-19-0126.1Hecht, C. W. & Cordeira, J. M. (2017). Characterizing Characterising Characterising the influence of atmospheric river orientation and intensity on precipitation distributions over North Coastal California. *Geophysical Research Letters*, *44*(17), 9048–9058. https://doi.org/10.1002/2017GL074179Hersbach, H., Bell, B., Berrisford, P., Hirahara, S., Horányi, A., Muñoz-Sabater, J., Nicolas, J., Peubey, C., Radu, R., Schepers, D., Simmons, A., Soci, C., Abdalla, S., Abellan, X., Balsamo, G., Bechtold, P., Biavati, G., Bidlot, J., Bonavita, M., … Thépaut, J. (2020). The ERA5 global reanalysis. *Quarterly Journal of the Royal Meteorological Society*, *146*(730), 1999–2049. https://doi.org/10.1002/qj.3803Hughes, M., Mahoney, K. M., Neiman, P. J., Moore, B. J., Alexander, M. & Ralph, F. M. (2014). The Landfall and Inland Penetration of a Flood-Producing Atmospheric River in Arizona. Part II: Sensitivity of Modeled Precipitation to Terrain Height and Atmospheric River Orientation. *Journal of Hydrometeorology*, *15*(5), 1954–1974. https://doi.org/10.1175/JHM-D-13-0176.1Kingston, D. G., Lavers, D. A. & Hannah, D. M. (2016). Floods in the Southern Alps of New Zealand: the importance of atmospheric rivers. *Hydrological Processes*, *30*(26), 5063–5070. https://doi.org/10.1002/hyp.10982Kingston, D. G., Lavers, D. A. & Hannah, D. M. (2021). Characteristics and large-scale drivers of atmospheric rivers associated with extreme floods in New Zealand. *International Journal of Climatology*, *February*, 1–17. https://doi.org/10.1002/joc.7415Lavers, D. A., Villarini, G., Allan, R. P., Wood, E. F. & Wade, A. J. (2012). The detection of atmospheric rivers in atmospheric reanalyses and their links to British winter floods and the large-scale climatic circulation. *Journal of Geophysical Research: Atmospheres*, *117*(D20), 1–13. https://doi.org/10.1029/2012JD018027Liu, X., Ma, X., Chang, P., Jia, Y., Fu, D., Xu, G., Wu, L., Saravanan, R. & Patricola, C. M. (2021). Ocean fronts and eddies force atmospheric rivers and heavy precipitation in western North America. *Nature Communications*, *12*(1), 1–10. https://doi.org/10.1038/s41467-021-21504-wNayak, M. A. & Villarini, G. (2017). A long-term perspective of the hydroclimatological impacts of atmo-

spheric rivers over the central United States. *Water Resources Research*, *53*(2), 1144–1166. https://doi.org/10.1002/2016WR019033Neiman, P. J., Ralph, F. M., Moore, B. J., Hughes, M., Mahoney, K. M., Cordeira, J. M. & Dettinger, M. D. (2013). The Landfall and Inland Penetration of a Flood-Producing Atmospheric River in Arizona. Part I: Observed Synoptic-Scale, Orographic, and Hydrometeorological Characteristics. *Journal of Hydrometeorology*, *14*(2), 460–484. https://doi.org/10.1175/JHM-D-12-0101.1Neiman, P. J., Ralph, F. M., Wick, G. A., Lundquist, J. D. & Dettinger, M. D. (2008). Meteorological Characteristics and Overland Precipitation Impacts of Atmospheric Rivers Affecting the West Coast of North America Based on Eight Years of SSM/I Satellite Observations. *Journal of Hydrometeorology*, *9*(1), 22–47. https://doi.org/10.1175/2007JHM855.1Neiman, P. J., Schick, L. J., Ralph, F. M., Hughes, M. & Wick, G. A. (2011). Flooding in Western Washington: The Connection to Atmospheric Rivers*. *Journal of Hydrometeorology*, *12*(6), 1337–1358. https://doi.org/10.1175/2011JHM1358.1Newell, R. E., Newell, N. E., Zhu, Y. & Scott, C. (1992). Tropospheric rivers? - A pilot study. *Geophysical Research Letters*, *19*(24), 2401–2404. https://doi.org/10.1029/92GL02916Newell, R. E. & Zhu, Y. (1994). Tropospheric rivers: A one-year record and a possible application to ice core data. *Geophysical Research Letters*, *21*(2), 113–116. https://doi.org/10.1029/93GL03113NIWA. (2008). *New Zealand Historic Weather Events Catalogue.* https://hwe.niwa.co.nz/event/August_2008_Canterbury_Flooding_and_North_I (2009). *New Zealand Historic Weather Events Catalogue.* https://hwe.niwa.co.nz/event/February_2009_New_ tropical_Cyclone_InnisNZ Herald. (2019). *Wild weather: Overnight deluge floods North Island roads, winds uproot trees in Coromandel.* https://www.nzherald.co.nz/nz/wild-weather-overnight-deluge-floods-north-island-roads-winds-uproot-trees-in-coromandel/YV6XTDAGGK47BTUJLRVWHNU5TY/?c_id=1&objectid= M. & Lu, M. (2019). A Novel Atmospheric River Identification Algorithm. *Water Resources Research*, *55*(7), 6069–6087. https://doi.org/10.1029/2018WR024407Porhemmat, R., Purdie, H., Zawar-Reza, P., Zammit, C. & Kerr, T. (2020). Moisture Transport during Large Snowfall Events in the New Zealand Southern Alps: The Role of Atmospheric Rivers. *Journal of Hydrometeorology*, *22*(2), 425–444. https://doi.org/10.1175/jhm-d-20-0044.1Prince, H. D., Cullen, N. J., Gibson, P. B., Conway, J. & Kingston, D. G. (2021). A climatology of atmospheric rivers in New Zealand. *Journal of Climate*, *34*(11), 4383–4402. https://doi.org/10.1175/JCLI-D-20-0664.1Ralph, F. M., Rutz, J. J., Cordeira, J. M., Dettinger, M., Anderson, M., Reynolds, D., Schick, L. J. & Smallcomb, C. (2019). A scale to characterize characterise characterise the strength and impacts of atmospheric rivers. *Bulletin of the American Meteorological Society*, *100*(2), 269–289. https://doi.org/10.1175/BAMS-D-18-0023.1Ralph, F. M, Dettinger, M. D., Cairns, M. M., Galarneau, T. J. & Eylander, J. (2018). Defining "Atmospheric River": How the Glossary of Meteorology Helped Resolve a Debate. *Bulletin of the American Meteorological Society*, *99*(4), 837–839. https://doi.org/10.1175/BAMS-D-17-0157.1Ralph, F. M, Neiman, P. J. & Rotunno, R. (2005). Dropsonde Observations in Low-Level Jets over the Northeastern Pacific Ocean from CALJET-1998 and PACJET-2001: Mean Vertical-Profile and Atmospheric-River Characteristics. *Monthly Weather*

Review, *133*(4), 889–910. https://doi.org/10.1175/MWR2896.1Ralph, F. M, Neiman, P. J. & Wick, G. A. (2004). Satellite and CALJET Aircraft Observations of Atmospheric Rivers over the Eastern North Pacific Ocean during the Winter of 1997/98. *Monthly Weather Review*, *132*(7), 1721–1745. https://doi.org/10.1175/1520-0493(2004)132<1721:SACAOO>2.0.CO;2Ralph, F. M, Wilson, A. M., Shulgina, T., Kawzenuk, B., Sellars, S., Rutz, J. J., Lamjiri, M. A., Barnes, E. A., Gershunov, A., Guan, B., Nardi, K. M., Osborne, T. & Wick, G. A. (2019). ARTMIP-early start comparison of atmospheric river detection tools: how many atmospheric rivers hit northern California's Russian River watershed? *Climate Dynamics*, *52*(7–8), 4973–4994. https://doi.org/10.1007/s00382-018-4427-5Reid, K. J., King, A. D., Lane, T. P. & Short, E. (2020). The Sensitivity of Atmospheric River Identification to Integrated Water Vapor Transport Threshold, Resolution, and Regridding Method. *Journal of Geophysical Research: Atmospheres*, *125*(20), 1–15. https://doi.org/10.1029/2020JD032897Reid, K. J., Rosier, S. M., Harrington, L. J., King, A. D. & Lane, T. P. (2021). Extreme rainfall in New Zealand and its association with Atmospheric Rivers. *Environmental Research Letters*, *16*(4). https://doi.org/10.1088/1748-9326/abeae0Salinger, M. J. (1980). New Zealand Climate: I. Precipitation Patterns. *Monthly Weather Review*, *108*(11), 1892–1904. https://doi.org/10.1175/1520-0493(1980)108<1892:NZCIPP>2.0.CO;2Shields, C. A., Rutz, J. J., Leung, L.-Y., Ralph, F. M., Wehner, M., Kawzenuk, B., Lora, J. M., McClenny, E., Osborne, T., Payne, A. E., Ullrich, P., Gershunov, A., Goldenson, N., Guan, B., Qian, Y., Ramos, A. M., Sarangi, C., Sellars, S., Gorodetskaya, I., … Nguyen, P. (2018). Atmospheric River Tracking Method Intercomparison Project (ARTMIP): project goals and experimental design. *Geoscientific Model Development*, *11*(6), 2455–2474. https://doi.org/10.5194/gmd-11-2455-2018Shu, J., Shamseldin, A. Y. & Weller, E. (2021). The impact of atmospheric rivers on rainfall in New Zealand. *Scientific Reports*, *11*(1), 5869. https://doi.org/10.1038/s41598-021-85297-0Shu, J., Shamseldin, A. Y., Weller, E. & Melville, B. W. (2021). *The role of Atmospheric rivers on monthly water availability and floods in New Zealand.* https://doi.org/10.1002/ESSOAR.10508631.1Sodemann, H. & Stohl, A. (2013). Moisture origin and meridional transport in atmospheric rivers and their association with multiple cyclones. *Monthly Weather Review*, *141*(8), 2850–2868. https://doi.org/10.1175/MWR-D-12-00256.1Tait, A. B. & Fitzharris, B. B. (1998). Relationships between New Zealand rainfall and southwest Pacific pressure patterns. *International Journal of Climatology*, *18*(4), 407–424. https://doi.org/10.1002/(SICI)1097-0088(19980330)18:4<407::AID-JOC256>3.0.CO;2-SZhang, Z., Ralph, F. M. & Zheng, M. (2019). The Relationship Between Extratropical Cyclone Strength and Atmospheric River Intensity and Position. *Geophysical Research Letters*, *46*(3), 1814–1823. https://doi.org/10.1029/2018GL079071Zhou, Y. & Kim, H. (2019). Impact of Distinct Origin Locations on the Life Cycles of Landfalling Atmospheric Rivers Over the U.S. West Coast. *Journal of Geophysical Research: Atmospheres*, *124*(22), 11897–11909. https://doi.org/10.1029/2019JD031218Zhu, Y. & Newell, R. E. (1994). Atmospheric rivers and bombs. *Geophysical*

Research Letters, *21*(18), 1999–2002. https://doi.org/10.1029/94GL01710Zhu, Y. & Newell, R. E. (1998). A Proposed Algorithm for Moisture Fluxes from Atmospheric Rivers. *Monthly Weather Review*, *126*(3), 725–735. https://doi.org/10.1175/1520-0493(1998)126<0725:APAFMF>2.0.CO;2